JOURNAL OF APPLIED POLYMER SCIENCE VOL. 21, 1597–1605 (1977)

Physical and Chemical Stress Relaxation of a Fluoroelastomer

EDWARD A. SALAZAR, JOHN G. CURRO, and KENNETH T. GILLEN,
Sandia Laboratories, Albuquerque, New Mexico 87115

Synopsis

Stress relaxation measurements were made at various temperatures on V-747-7, a commercial high-temperature rubber formulation from the Parker Seal Company. The data were analyzed by separating the chemical and physical relaxation processes by a method described in an earlier publication. The chemical relaxation process was found to be Arrhenius with an activation energy of 35.7 kcal/mole. The results allow us to predict the relative useful lifetimes of this material up to approximately 320°C.

INTRODUCTION

There are a great variety of polymers based on a carbon chain backbone which utilize high fluorine substitution to obtain outstanding resistance to the effects of heat and to a variety of active chemicals and solvents. The classic example of this is poly(tetrafluoroethylene) (TFE) which has a carbon chain completely substituted with fluorine. While this material possibly represents the ultimate for this class of polymers in terms of ability to resist thermal or chemical degradation, it is a stiff, high-modulus thermoplastic which is subject to distortion at high temperature, particularly under stress. Direct chemical descendants of TFE plastic resins are the fluoroelastomers. These highly crosslinked systems were developed to meet the above requirements of high-temperature stability and good solvent and chemical resistance coupled with the added benefits of flexibility and resiliency. Some of the most important high-temperature rubbers are based on formulations using Viton (trademark of E. I. du Pont De Nemours) or Fluorel (trademark of Minnesota Mining & Manufacturing) (copolymers of vinylidene fluoride and hexafluoropropylene) fluoroelastomers.

A recent rubber formulation with exceptional high-temperature properties is V-747-7 formulated by the Parker Seal Company. The purpose of this investigation is to estimate the long-term high-temperature properties of this formulation. This is accomplished by performing stress relaxation measurements[1,2] at elevated temperatures and extrapolating to long times at lower temperatures using methods previously described.[3] We will show that these data can be used to predict the useful lifetime of this rubber, and in a later paper the more complex case of O-ring lifetimes will be addressed.

Previous stress relaxation and creep measurements on fluorocarbons include studies on Viton ECD-006,[4,5] Halar,[5] Tefzel,[5] Viton A,[6,7] and Viton B.[8,9] For

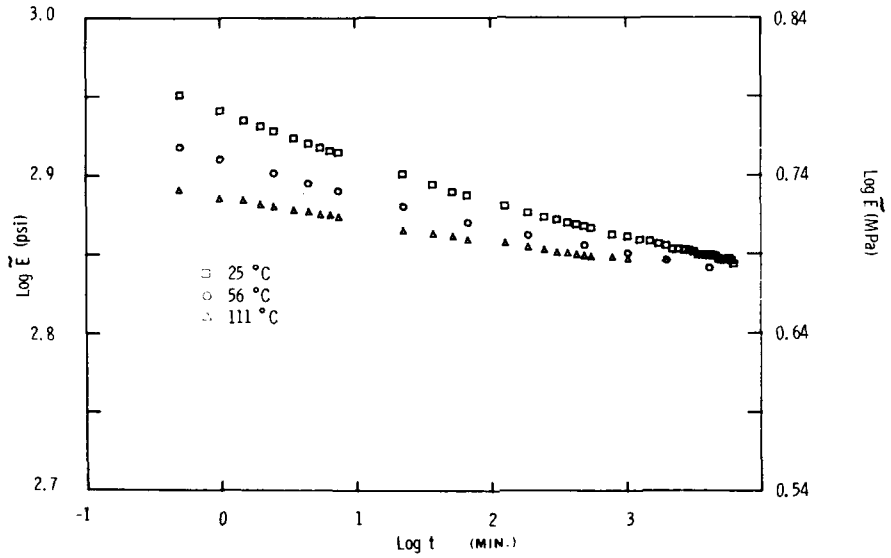

Fig. 1. Typical low-temperature stress relaxation data for Viton.

our purposes, perhaps the most pertinent of these articles is the study of Viton B by Kalfayan et al.[9] This study contains extensive stress relaxation data at elevated temperatures and various environments. However, comparison with our stress relaxation results indicate that the ultralow compression-set material in the present study appears to be superior to their Viton B material. In addition, Kalfayan et al.[9] considered only the chemical relaxation contributions to their stress relaxation process. In the present study, both the physical and chemical stress relaxation are considered in the analysis.

EXPERIMENTAL AND RESULTS

Stress relaxation was measured on fluorocarbon rubber (Viton) obtained from the Parker Seal Company under product designation V-747-7. This material is an ultralow compression-set fluoroelastomer formulated from du Pont Viton E 60 C or from 3M Fluorel 2170, equivalent copolymers of vinylidene fluoride and hexafluoropropylene. Test specimens were 7.62-cm long, 0.635-cm wide, and approximately 0.22-cm thick. The experiment was divided into two temperature ranges: low temperature (~25°C to 111°C) and high temperature (263°C to 319°C), using two different test procedures.

The low-temperature tests were made on a stress relaxation apparatus which interfaces with a PDP-11-10 computer for automatic data acquisition. The specimens were mounted in the test apparatus at room temperature with no stress applied. After the temperature was raised and allowed to equilibrate over a period of 15 min to ±0.2°C, the specimens were pulled to ~20% strain at a rate >20 in./min. Loads were monitored on a 0- to 10-lb tension transducer (Sensotec Model LKFA-30) and the strain measured with a cathetometer. Complete details on the test apparatus have been presented previously.[3] Typical low-temperature test data are shown in Figure 1, where the reduced modulus is plotted as a function of the time for various temperatures. The reduced modulus is calculated from the equation derived from rubber elasticity theory:[1]

$$\tilde{E} = \left(\frac{3\sigma}{\lambda - 1/\lambda^2}\right)\frac{T_0}{T}\left[1 + \alpha_v(T - T_0)\right] \quad (1)$$

where σ is the stress, λ is the stretch ratio, α_v is the volumetric coefficient of expansion, and T is the absolute temperature. The reference state, T_0, is chosen to be 298°K. The volumetric coefficient of expansion, α_v, is taken to be $3\alpha_L$, where α_L is the linear coefficient of expansion (α_L = 205 ppm/°C). For repeated runs at a single temperature, the shape of the low-temperature curves were almost identical; scatter in the magnitude due to slight uncertainties in the strain of the sample was typically less than 5%.

Due to temperature limitations on the stress relaxation apparatus, the high-temperature tests (263°C to 319°C) were conducted on an Instron testing machine using an Instron G-30 environmental chamber capable of maintaining temperatures to better than ±1°C over the operating range (manufacturer's data). The oven temperature was raised to the temperature of interest, and sufficient time was allowed so that all clamps and fixtures reached thermal equilibrium. The specimens were then introduced within a 3-min period, followed by another 3 min necessary to reestablish temperature equilibrium. They were then pulled to approximately 10% strain as estimated from the cross-head travel. The stress relaxation results then allow us to obtain the reduced modulus in a manner similar to the low-temperature results. However, as will become clear later, we are primarily interested in the shape of the stress relaxation curves.

The linear coefficient of expansion used in the analysis of the data was determined on a Thermal Mechanical Analyzer, Perkin–Elmer Model TMS-1, at a testing rate of 5°C/min.

DISCUSSION

It is well known[1] that in a strained elastomer, two relaxation mechanisms exist. These are known as physical and chemical stress relaxation. Physical relaxation involves physical processes such as diffusion of polymer chain units or movement of entanglements, whereas chemical relaxation involves the breaking of covalent bonds. These two processes are expected to have different temperature dependencies, hence an analysis of the stress relaxation of rubber necessitates a separation of these two effects. This problem has been discussed previously.[3]

In this work on Viton, we assume that in the low-temperature range (25–111°C), no appreciable chemical relaxation occurs over the time scale of the experiment, which is about 100 hr. With this assumption, which will be verified later, the low-temperature data are analyzed using coventional time–temperature superposition techniques.[2] This allows us to estimate the amount of physical relaxation occurring in each of the high-temperature experiments. These physical contributions are then subtracted from the total stress relaxation curves at the high temperatures, thus isolating the chemical effect.

The low-temperature stress relaxation data on Viton were shifted using the usual time–temperature superposition technique.[2] This leads to the master curve shown in Figure 2, with the reference temperature T_0 = 25°C. The log

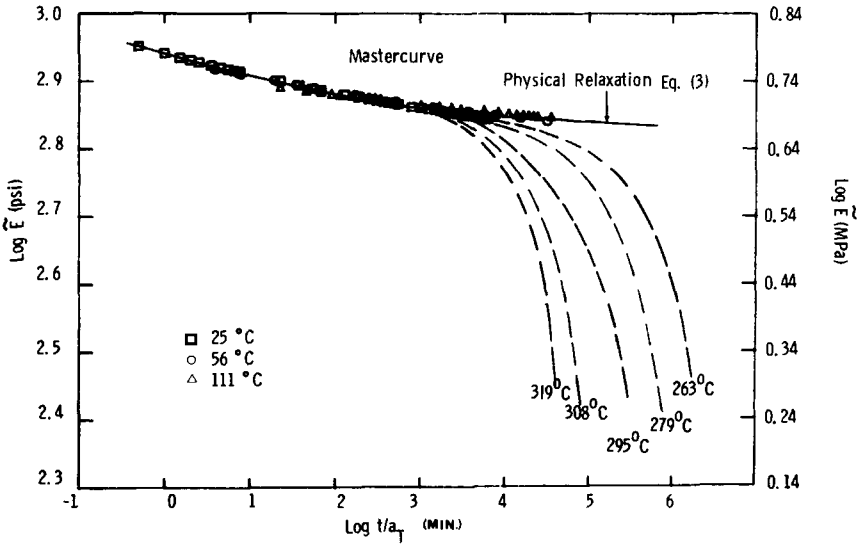

Fig. 2. Typical time–temperature shifted stress relaxation data for Viton.

of the shift factor a_T is plotted in Figure 3 for various experimental temperatures. It should be pointed out that the uncertainties expected in the time–temperature shift factors of the data in this work are large, because the slopes of the stress relaxation–time curves are small. These uncertainties are represented approximately by the radii of the circles. Even though these shift factors are subject to fairly large uncertainties, the resulting master curve in Figure 2 is much less sensitive to these uncertainties. Also shown in Figure 3 is a least-squares fit of the WLF equation[2] to the data. Even though this equation is subject to large uncertainties, it can be shown that these uncertainties do not affect the final results significantly. The high-temperature data were now shifted horizontally according to this WLF equation. These curves were also slightly shifted in the vertical direction so they merge at the shortest times (20 sec) with the mastercurve. Because of the random scatter always present in stress relaxation data (~10% in our high-temperature runs), these shifts were necessary to assure internal consistency of the data, i.e., zero chemical reaction at time zero. This assumption will be verified later. The resulting high-temperature curves are shown in Figure 2. It is obvious that at long times, significant deviations due to chemical relaxation occur. As has been pointed out previously, these departures from the physical relaxation curve can be used to estimate the overall kinetics of the reaction leading to chemical stress relaxation. The expression used to estimate this effect is given by[3]

$$\log (\nu/\nu_0) \cong \log \tilde{E}(t, T, \nu) - \log \{\tilde{E}_e(\nu_0)\,[1 + (\tau a_T/t)^m]\} \qquad (2)$$

where $\tilde{E}$ is the reduced relaxation modulus which depends on the time t, the absolute temperature T, and crosslink density ν. The initial crosslink density is ν_0, so that ν/ν_0 represents the fraction of initial crosslinks remaining at time t. The second term on the right-hand side of this equation is a semiempirical representation of the physical stress relaxation at a fixed, initial crosslink density

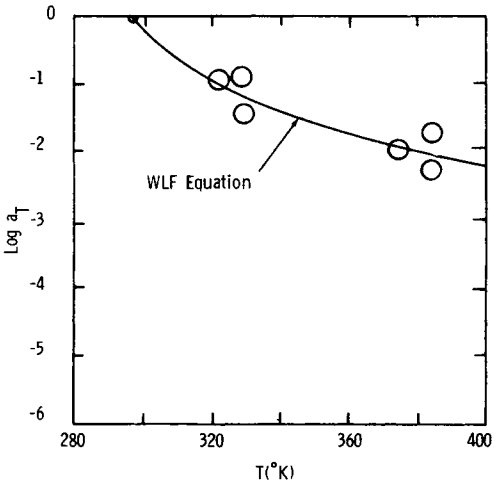

Fig. 3. Time–temperature shift factors for Viton.

ν_0; $\tilde{E}_e$ is the reduced equilibrium modulus; and τ and m are material parameters.

The physical relaxation parameters $\tilde{E}_e$, τ, and m were determined for Viton from a least-squares fit of the low-temperature master curve to the equation

$$\tilde{E} = \tilde{E}_e[1 + (\tau a_T/t)^m] \tag{3}$$

An equation of this form is known to be a good representation of the physical stress relaxation process.[3,10,11] The resultant physical relaxation parameters are shown in Table I, and the curve plotted from eq. (3) with these parameters is also shown in Figure 2. The above allows us to calculate the second term on the right-hand side of eq. (2); and since the first term on the right-hand side can be obtained from the high-temperature stress relaxation data in Figure 2, we can now obtain values of log ν/ν_0 versus time at the high temperatures. This leads to the results shown in Figure 4.

It is now possible to estimate the crosslink density as a function of time at other arbitrary temperatures. First, let us assume that the rate equation for the crosslink density is of the general form

$$\frac{d(\nu/\nu_0)}{dt} = kf(\nu/\nu_0) \tag{4}$$

where k is a rate constant and f is some arbitrary function of the crosslink density. Further, let us assume that the rate constant has Arrhenius temperature dependence

$$\log k = \log A - (H/2.303RT) \tag{5}$$

TABLE I
Physical Relaxation Parameters for Viton

C_1	C_2	$\tilde{E}_e$, psi	m	τ, min
3.50	67.2	618	0.122	0.000727

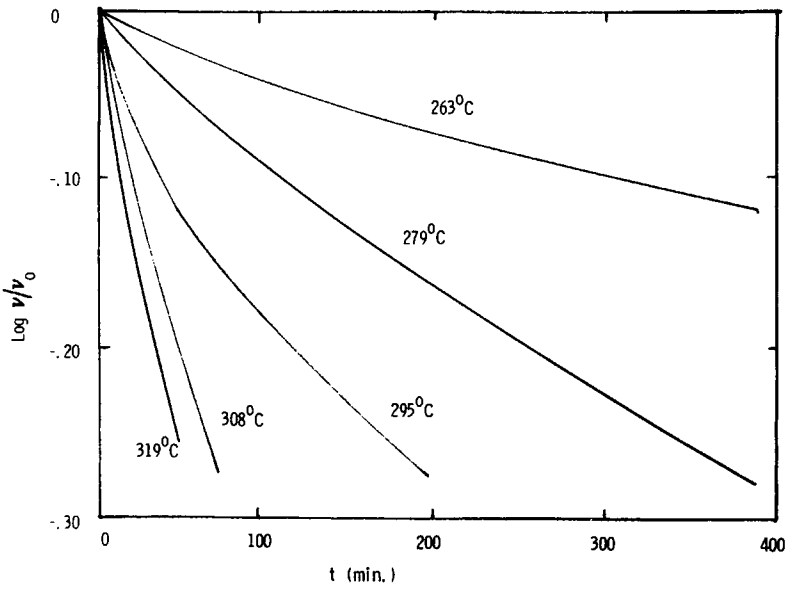

Fig. 4. Plot at a number of temperatures of the fraction of initial crosslinks remaining as a function of time.

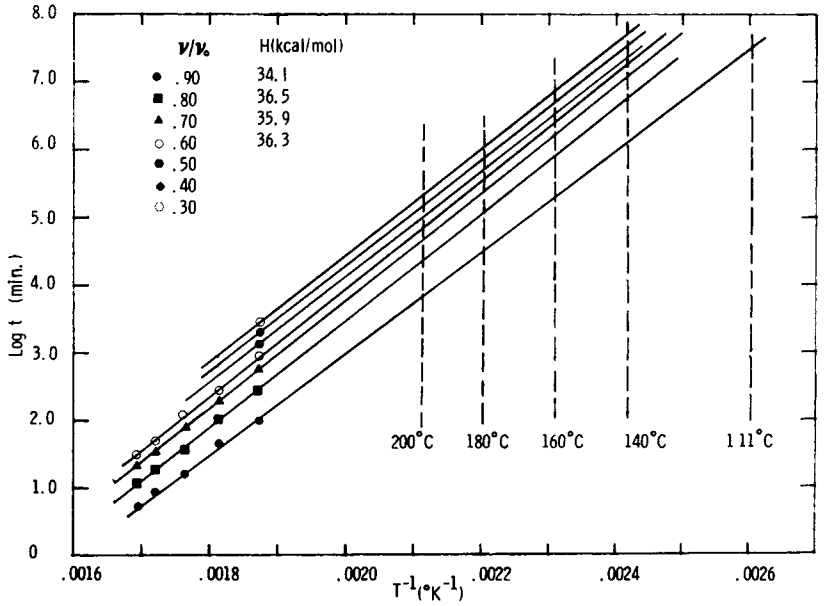

Fig. 5. Plot of inverse temperature vs. log of the time required for chemical relaxation to reduce the fraction of initial crosslinks ν/ν_0 to constant values.

where A is the frequency factor and H is the activation energy. If eq. (4) is integrated and eq. (5) is used for the rate constant, then the following equation is obtained:

$$\log t = \log F(\nu/\nu_0) + (H/2.303RT) \tag{6}$$

where for constant strain levels and constant composition, F is a function of the crosslink density only:

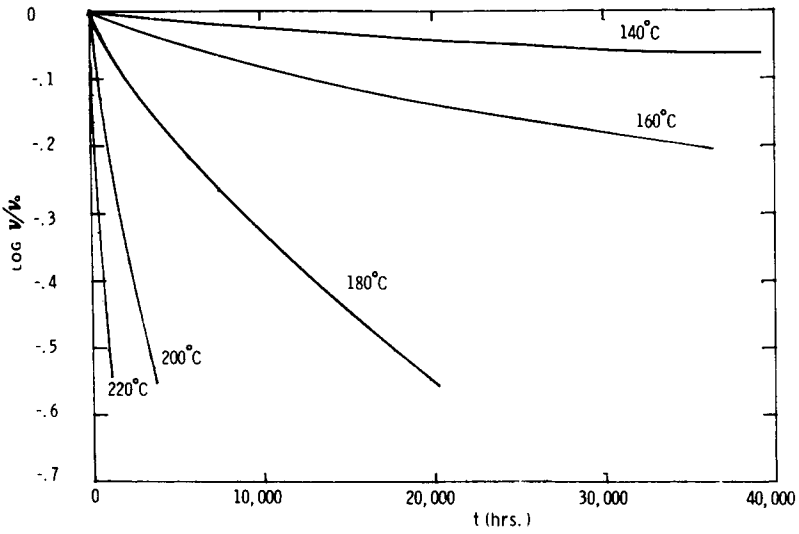

Fig. 6. Calculated change in ν/ν_0 vs. time for a number of temperatures.

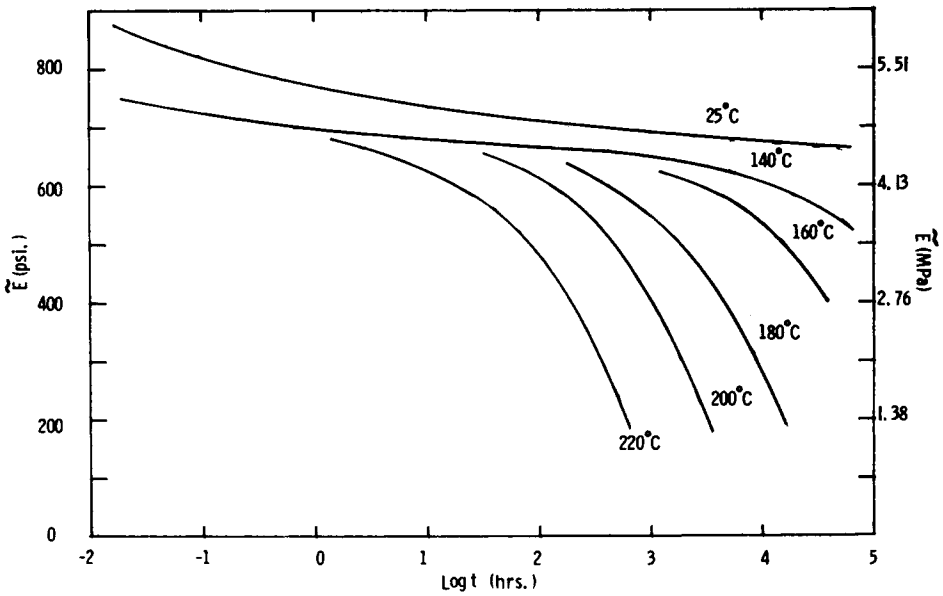

Fig. 7. Predicted stress relaxation modulus for Viton at various temperatures.

$$F(\nu/\nu_0) = \mathrm{A}^{-1} \int_1^{\nu/\nu_0} \frac{dx}{f(x)} \tag{7}$$

Thus, if $\log t$ at a fixed conversion $(1 - \nu/\nu_0)$ is plotted versus T^{-1}, a straight line should be obtained whose slope is $H/2.303R$. Furthermore, H should be independent of the conversion chosen. The plot for our Viton data is shown in Figure 5. It can be seen that the resulting lines are approximately straight and parallel, which supports the use of eqs. (4)–(6). The average activation energy was found to be 35.7 kcal/mole. The crosslink density kinetics at lower temperatures can

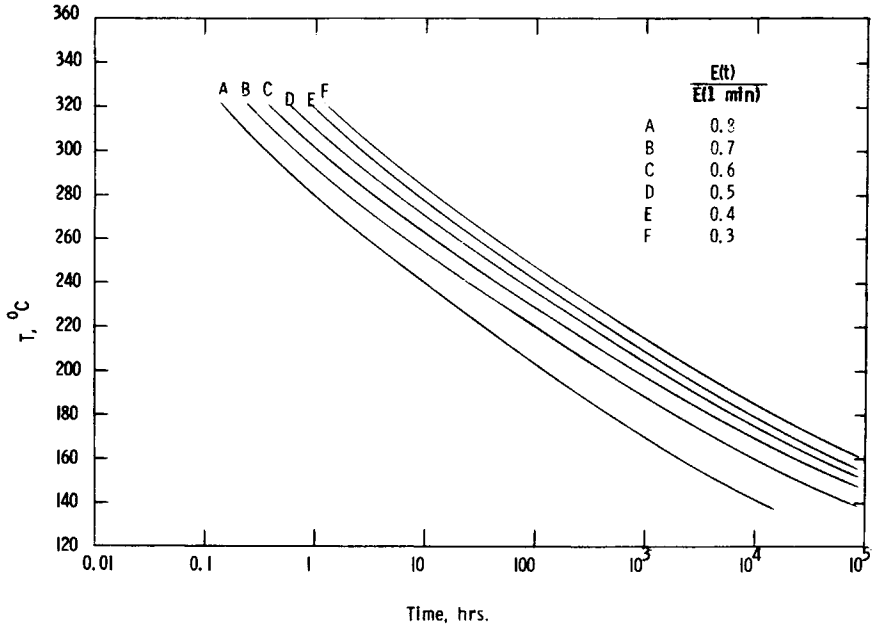

Fig. 8. Time required to reach a given relaxation modulus ratio for Viton at various temperatures.

now be found by extrapolation of these lines. As an illustration, extrapolations were made to temperatures of 140°, 160°, 180°, and 200°C. Since data were taken for conversions above 40% only for the 279°C run, the extrapolations for higher conversions were made using straight lines through the 279°C data points, with a slope determined from the average activation energy of 35.7 kcal/mole. The resultant estimated curves are shown in Figure 6.

The stress relaxation curves at these arbitrary temperatures can now be constructed from eq. (2) using the values ν/ν_0 and the physical relaxation parameters obtained above. These predictions are shown in Figure 7.

It is now possible to check our assumptions that no chemical relaxation occurs in the temperature range of 25° to 111°C over the time scale of the experiment (~100 hr) and that chemical relaxation is minimal at the earliest time (~20 sec) in the high-temperature runs. By determining log ν/ν_0 versus time at 111°C (similar to Fig. 6), we find $\nu/\nu_0 \approx 1.0$ at 100 hr, thereby justifying the first assumption. Similarly, ν/ν_0 is estimated to be ≈ 0.99 after 20 sec at 319°C, thus justifying the second assumption.

It may be argued that perhaps significant chemical relaxation occurred during the 6-min period required for specimen mounting and temperature equilibrium. To address this point, stress–strain measurements were made on specimens aged at 350°C for 30 min. For 10% strain, a difference in stress of less than 1% was observed between the aged and unaged specimens. This indicates that in the 6-min equilibration period, no net change in crosslink density occurs. Thus, although crosslinks may be breaking in the unrestrained specimen, an approximate equal number of crosslinks are reforming. After stretching, of course, any reformed crosslinks are not observed since their equilibrium position is for the stressed state; and hence, they do not contribute to maintaining the stress.

It is interesting to compare our results on Viton V-747-7 with the results obtained on Viton B by Kalfayan and co-workers.[9] These workers found activation energies ranging from 16 to 20 kcal/mole for Viton B in air, whereas our average measured activation energy for Parker's V-747-7 in air was found to be 35.7 kcal/mole. This larger activation energy is the reason that the V-747-7 is more stable at high temperature than Viton B.

Since V-747-7 is a very stable elastomer at high temperatures, it is useful in many applications such as O-rings and seals. In order to estimate the useful lifetime of this material in various applications, we have crossplotted the data of Figure 2 and the predictions shown in Figure 7. This appears in Figure 8 where we have plotted against temperature the time required for the relaxation modulus ratio $\tilde{E}(\tau)/\tilde{E}$ (1 min) to reach the values of 0.8, 0.7, 0.6, 0.5, 0.4, and 0.3.

In this work, we have determined the relaxation modulus which is a material property. The use of this material function for a specific application necessitates the solution of the equations of motion with boundary conditions appropriate to the geometry of interest. Other complicating factors can also exist such as weight loss and thermal expansion effects. These factors will be considered in a future paper where we analyze the important and practical applications of aging of O-rings.

This work was supported by U.S. Energy Research & Development Administration.

References

1. A. V. Tobolsky, *Properties and Structure of Polymers,* Wiley, New York, 1960.
2. J. D. Ferry, *Viscoelastic Properties of Polymers,* Wiley, New York, 1960.
3. J. G. Curro and E. A. Salazar, *J. Appl. Polym. Sci.,* **19,** 2571 (1975).
4. L. E. Himelreich, *SAMPE Technology in Transition,* Proceedings of 20th SAMPE Symposium, 1975, p. 345.
5. P. L. Merz, *SAMPE Technology in Transition,* Proceedings of 20th SAMPE Symposium, 1975, p. 356.
6. K. W. Scott, R. V. Allen, R. D. Gates, and M. Morton, U.S. Dept. of Commerce Office of Technical Service, P.B. Report 155,233, 1960.
7. A. S. Novikov, F. S. Tolstuklina, and N. N. Kolesniknikova, Proceedings of Rubber Tech. Conf., London, 1962.
8. N. Tuyendyk, *Rev. Gen. Cautchotec Plastiques,* **43,** 981 (1966).
9. S. H. Kalfayan, R. H. Silver, A. A. Maggeo, and S. T. Liu, *Jet Propulsion Lab. Quart. Tech. Rev.,* **2,** 32 (1972).
10. R. Chasset and P. Thision, in *Proc. Int. Conf. Noncrystalline Solids,* North-Holland, Amsterdam, 1965, p. 345.
11. D. Plazek, *J. Polym. Sci.,* **A2,** 811 (1964).

Received December 8, 1975
Revised May 4, 1976